J. Fluid Mech. (2000), *vol.* 405, *pp.* 111–129. Printed in the United Kingdom

Marangoni convection. Part 2. A cavity subject to point heating

By M. HAMED AND J. M. FLORYAN
Department of Mechanical and Materials Engineering, The University of Western Ontario, London, Ontario, N6A 5B9, Canada

(Received 6 October 1997 and in revised form 6 October 1999)

Marangoni convection in a cavity subject to point (concentrated) heating has been investigated. The analysis includes the complete effects of the interface deformation. The results determined for large Biot and zero Marangoni (zero Prandtl) numbers show that steady convection may exist only for a limited range of Reynolds numbers *Re* (bounded from above and from below), and for capillary numbers *Ca* and cavity lengths *L* smaller than certain critical values. The main factor limiting the existence of steady convection involves the interface approaching the bottom of the cavity. Unsteady analysis shows that when the conditions guaranteeing the existence of steady convection are not met, an interface rupture process sets in leading, eventually, to the formation of a dryout at the bottom of the cavity. The initial stages of the rupture process are characterized by a rapidly accelerating growth of the interface deformation. The critical values of *Re*, *Ca* and *L*, which guarantee the existence of steady convection, are mutually dependent and change with the heating rate; they reach a minimum for instantaneous heating. Too rapid heating produces an oscillatory transient which always decays in the range of parameters studied.

1. Introduction

This paper reports results of an analysis of the various phenomena that can be induced by the thermocapillary effect. The understanding of these phenomena and the development of techniques for their control are important in many areas of technology, specifically in zero-gravity containerless material processing and in laser cutting. Because of the complexity of problems found in applications, we shall focus our attention on a simple reference problem consisting of a liquid contained in a cavity open from above, with the free upper surface subject to an externally imposed non-uniform heating, and with gravity absent. A complete understanding of the dynamics of this simple system forms a convenient starting point for the analysis of real systems. A detailed description of the model problem together with a review of the relevant literature is given in Part 1 (Hamed & Floryan 2000). The present work uses the same model problem and the same notation.

Floryan & Chen (1994) analysed the model problem referred to above and demonstrated that the response of the liquid strongly depends on the type of external heating. An infinite liquid layer may exist only when the external temperature field satisfies restrictive existence conditions. Violation of these conditions leads to a large interfacial deformation leading (possibly) to rupture of the layer. When a finite layer is subject to such a heating, a large deformation occurs leading to the rupture of the layer if the cavity is made sufficiently long. Tan, Bankoff & Davis (1990) considered an infinite layer subject to periodic heating and used the long-wavelength approximation to predict the interface rupture. Burelbach, Bankoff & Davis (1990) confirmed these predictions experimentally. Since the existence conditions are very restrictive and unlikely to be satisfied in practical applications, it is of interest to study the response of the liquid subject to non-uniform heating under conditions leading to a potentially large deformation (i.e. when the existence conditions are violated).

The behaviour of the liquid when the cavity sidewalls are differentially heated and the external temperature varies linearly along the interface is described in Part 1. Steady convection exists for a limited range of Reynolds numbers *Re* (bounded from below), and for capillary numbers *Ca* and cavity lengths L smaller than certain critical values. The tangency condition, where the interface becomes tangential to the hot wall, was identified as the limiting factor for the existence of a continuous interface connecting two specified contact points. Violation of this condition suggests possible formation of a dryout on the hot wall in real systems. Time-dependent simulations showed that the tangency condition determines the limit points for the steady response of the system. When the heating is applied too rapidly, a large initial transient is produced resulting in a large deformation and, possibly, leading to the violation of the tangency condition before the limit point is reached. This transient can be eliminated by reducing the heating rate. For a certain range of *Ca* and *Re* the system admits two solutions, a steady one and an oscillatory one. The oscillatory mode consists of the steady mode with a simple harmonic sloshing motion superposed on it.

It is of interest to determine how the response of the system changes when another type of heating is applied. This paper reports results of such an investigation with the liquid subject to point heating. This particular form of heating has been selected because it mimics the heating produced by a laser. The corresponding temperature distribution in the gas phase has been assumed of Gaussian form (following Floryan & Chen 1994), i.e.

$$T_g(x) = 8\mathrm{e}^{-x^2}. \tag{1}$$

This heating does not satisfy the existence conditions (Floryan & Chen 1994) and thus the interface is expected to undergo large deformations resulting, possibly, in its rupture. We shall demonstrate that steady convection may exist only for a limited range of *Re*, *Ca* (both are defined in the same manner as in Part 1) and L, and that the factor limiting its existence involves the interface approaching the bottom of the cavity. We shall also demonstrate that when the conditions guaranteeing the existence of steady convection are not met, an interface rupture process sets in, leading eventually to the formation of a dryout at the the bottom. The nature of the factor limiting the existence of the continuous interface in the present case is thus different from the one identified for the cavity with differentially heated sidewalls. It is further of interest to note that point heating does not induce any oscillatory convection for the range of parameters analogous to that studied for the cavity with differentially heated sidewalls.

2. Discussion of results

All numerical results presented in this section have been obtained using the algorithm described in Part 1. The error bounds and the grid densities used in the present study are similar to those used in the companion paper and have been determined through analogous grid convergence studies. Spot checking and verification of the results have also been carried as in the companion paper.

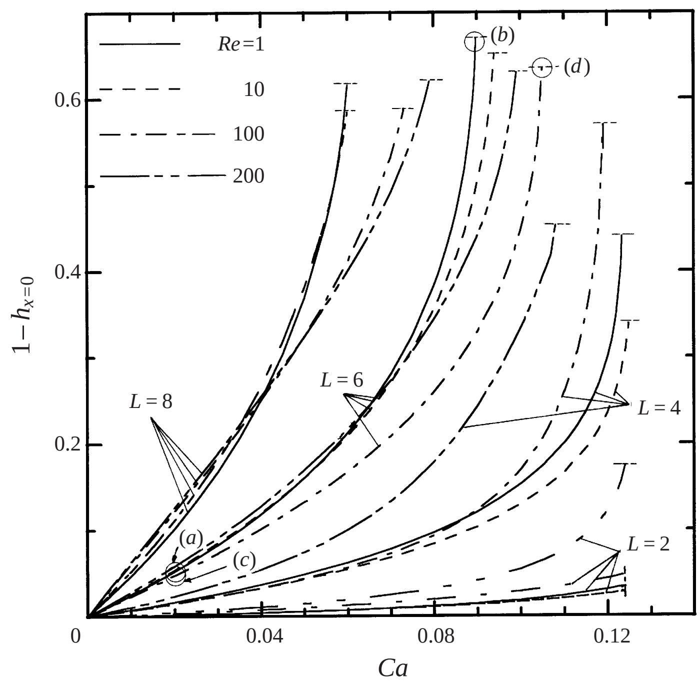

FIGURE 1. Interface deformation at $x = 0$ (maximum deformation) as a function of capillary number Ca. The flow and deformation patterns corresponding to points (*a–d*) are shown in figure 2.

In order to simplify the following discussion, we shall consider only the case of Marangoni number $Ma = 0$ (Prandtl number $Pr = 0$) and Biot number $Bi = \infty$, as in Part 1. The first condition limits our results to highly conductive liquids, such as liquid metals, where conductive heat transport dominates over convective heat transport. The second condition implies a very high heat transfer coefficient in the gas phase, which makes the temperature of the interface effectively equal to the temperature of the gas phase.

2.1. *Steady-state response*

As a first step, we shall determine the steady response of the liquid subject to surface heating corresponding to the temperature distribution in the gas phase given by (1). The sidewalls are assumed to have temperatures $T_L = T_R = T_g(\pm\frac{1}{2})$. Rivas (1991) simulated point heating by assuming a Gaussian distribution of heat flux. His results are limited to non-deformable interfaces and long cavities.

Figure 1 illustrates the evolution of the interface deformation at $x = 0$ as a function of the capillary number Ca for the cavity lengths $L = 2$, 4, 6, 8 and for the Reynolds numbers $Re = 1$, 10, 100, 200, respectively. This particular location along the interface has been selected because it corresponds to the maximum interface deformation induced by the point heating. The deformation curves were obtained by repeating calculations with Ca increasing in steps as small as $\Delta Ca = 0.0001$ until a critical value Ca_{cr} was identified above which no steady solutions were found. The reader may recall that increasing Ca corresponds to the interface becoming progressively 'softer'. In all cases the flow pattern was symmetric with respect to the centreline of the cavity (i.e. with respect to $x = 0$). It can be seen that as Ca increases,

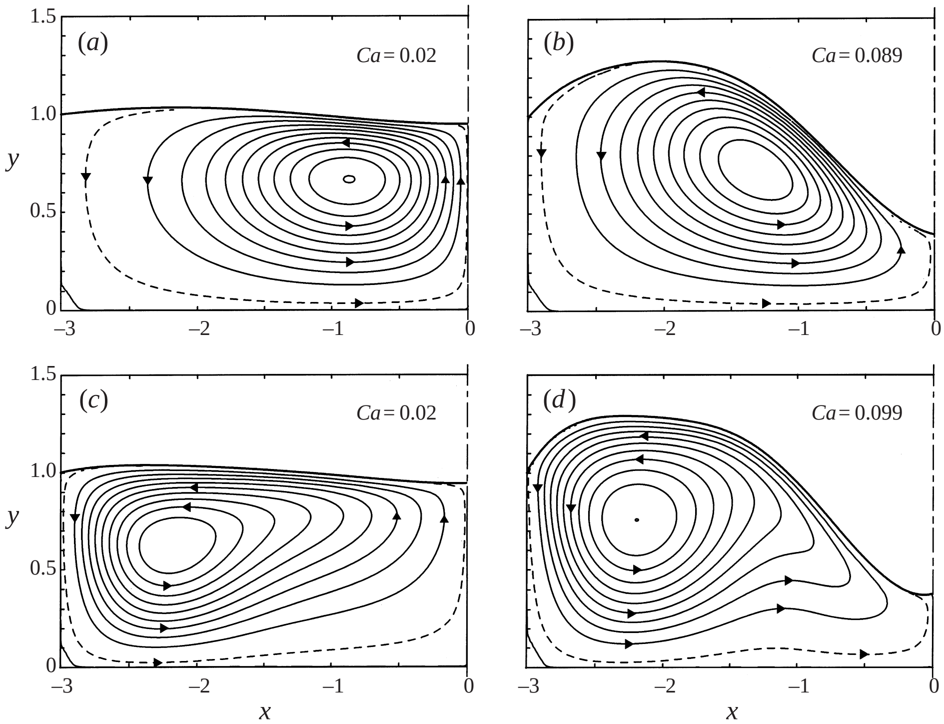

FIGURE 2. The evolution of the flow and deformation patterns as a function of capillary number Ca for $L = 6$, (a,b) $Re = 1$, (c,d) $Re = 200$. $(a–d)$ correspond to points $a–d$ on figure 1, respectively. Only the left side of the cavity is shown due to the symmetry of the flow. Contour lines are shown every 10% of ψ_{max} (solid lines). Dashed lines show 1% of ψ_{max}. In $(a–d)$ $|\psi|_{max}$ = 1.0614, 1.1269, 0.5703, 0.7171, respectively.

the maximum deformation increases at a rapidly accelerating rate. The form of the curves suggests that the deformation either becomes unbounded for $Ca > Ca_{cr}$, or the system reaches a limit point for $Ca = Ca_{cr}$, with Ca_{cr} being a function of both L and Re. We shall demonstrate in the next section that the latter is true.

It is difficult to correlate the variations of Ca_{cr} with Re because they are affected by the cavity length L. For example, for $L = 4$ this relation is non-monotonic and Ca_{cr} increases with Re increasing from $Re = 1$ to 10, and then it decreases with further increase of Re. For $L = 6$, Ca_{cr} keeps increasing for much higher values of Re and begins to decrease only after $Re > 100$. For $L = 8$, this relation becomes monotonic and Ca_{cr} increases with Re in the whole range of parameters studied. We shall come back to this question during discussion of the effects of the cavity length.

The evolution of the interface and the flow patterns are shown in figure 2(a,b) for $L = 6$, $Re = 1$ and in figure 2(c,d) for $L = 6$, $Re = 200$. The convection pattern consists of two large dominant vortices, each being the mirror image of the other. It can be seen that the locations of the centres of the vortices are marginally influenced by variations of Ca. Comparison of the figures shows that as Re increases the centres of the recirculating vortices move towards the sidewalls with the interface becoming progressively steeper there. The cores of the vortices become approximately inviscid and the vorticity inside becomes constant for higher values of Re. Such vortices are well described by the model proposed by Batchelor (1956). The local minimum

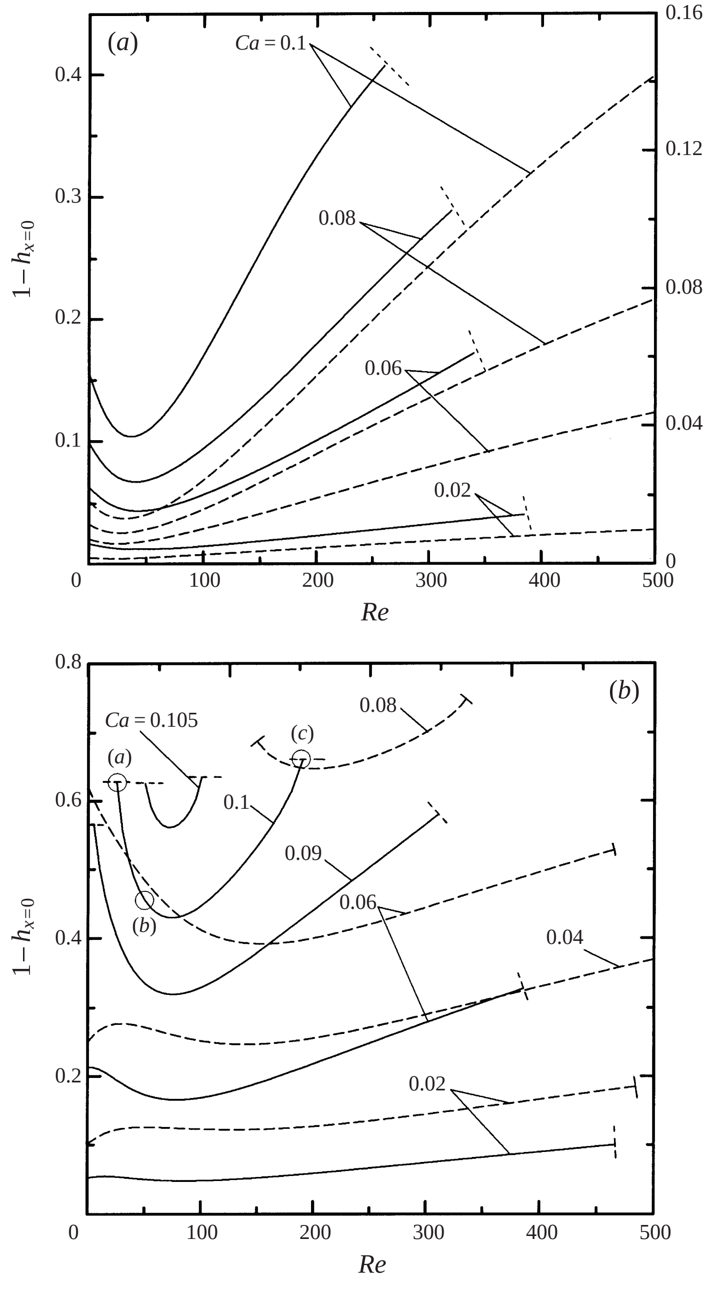

FIGURE 3. Interface deformation at $x = 0$ (maximum deformation) as a function of Reynolds number Re for (*a*) the cavity length $L = 2$ (dashed lines; right axis) and $L = 4$ (solid lines; left axis), and (*b*) the cavity length $L = 6$ (solid lines) and $L = 8$ (dashed lines).

pressure associated with the vortex core causes flattening of the interface above the vortex at $Re = 200$ (see figure 2*c, d*) and a local depression at higher Re (not shown).

Figures 3(*a*) and 3(*b*) illustrate the evolution of the interface deformation as a function of the Reynolds number Re for $L = 2$, 4 and 6, 8, respectively, and for various values of the capillary number Ca. It can be seen that as the Reynolds

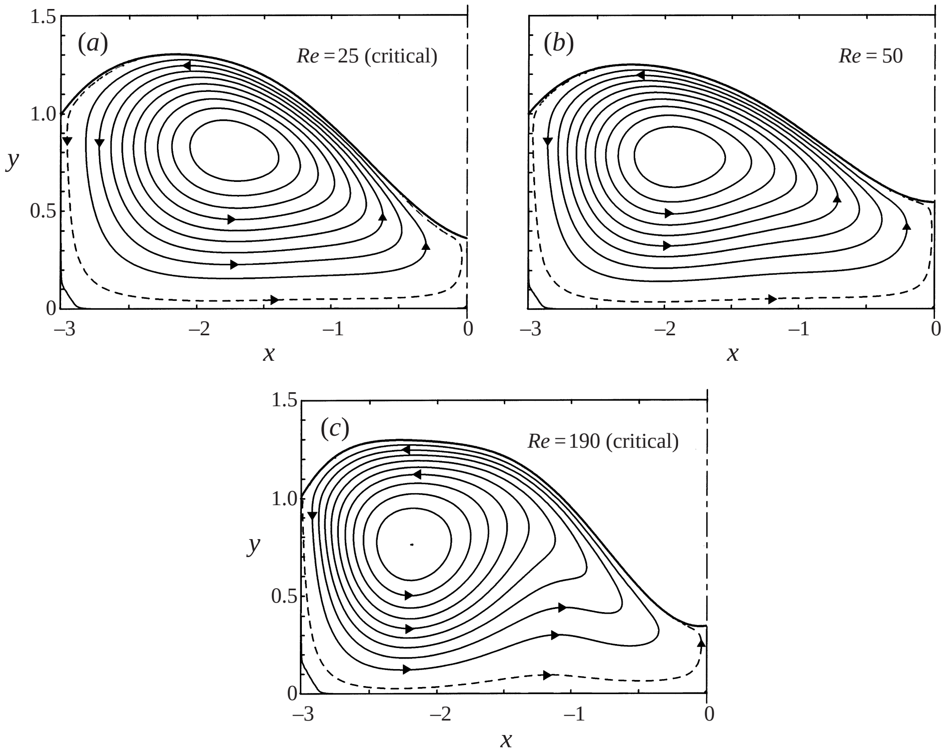

FIGURE 4. The evolution of the flow and deformation patterns as a function of Reynolds number Re for $Ca = 0.1$, $L = 6$. (a–c) correspond to points (a–c) in figure 3(b), respectively. Only the left side of the cavity shown due to the symmetry of the flow. Contour lines are shown every 10% of ψ_{max} (solid lines). Dashed lines show 1% of ψ_{max}. In (a–c) $|\psi|_{max} = 1.0879$, 0.9243, 0.7324 respectively.

number increases the deformation initially decreases, reaches a minimum, and then begins to increase until a limit point is reached (if such a limit point exists in the range of Re of this study, i.e. for $0 \leqslant Re \leqslant 500$). This non-monotonicity is associated with a change in the pattern of surface pressure distribution from the viscosity-dominated (creeping flow) one to an almost inviscid one dominated by the inertial effects. This transition occurs at lower Re in longer cavities and thus the non-monotonicity of the interface deformation is more pronounced in longer cavities for the same Re. We shall discuss this issue again later in the text. For $L = 2$ (figure 3a) steady solutions exist for all values of Re (with $Re \leqslant 500$). For $L = 4$ (figure 4) steady solutions do not exist if $Re > Re_{cr,a}$. The value of $Re_{cr,a}$ is a function of Ca and it decreases with an increase of Ca. When $L = 6$ and $L = 8$ (figure 3b), the range of Re for which steady solutions exist becomes bounded from below as well as from above, i.e. $Re_{cr,b} < Re < Re_{cr,a}$. This range becomes narrower as Ca increases. It will be shown in the next section that this range defines the limit points for steady solutions. The reader may also note that the change of L from 2 to 4 increases the deformation by a factor of 10, further increase of the cavity length to $L = 6$ increases the deformation by an additional factor of 3–4, and the change to $L = 8$ increases the deformation by another factor of 3–4.

The evolution of the flow field and the interface deformation patterns as a function of Re are illustrated in figure 4 for $L = 6$, $Ca = 0.1$. An initial reduction followed by an increase of the deformation as Re increases are clearly visible. This non-monotonicity

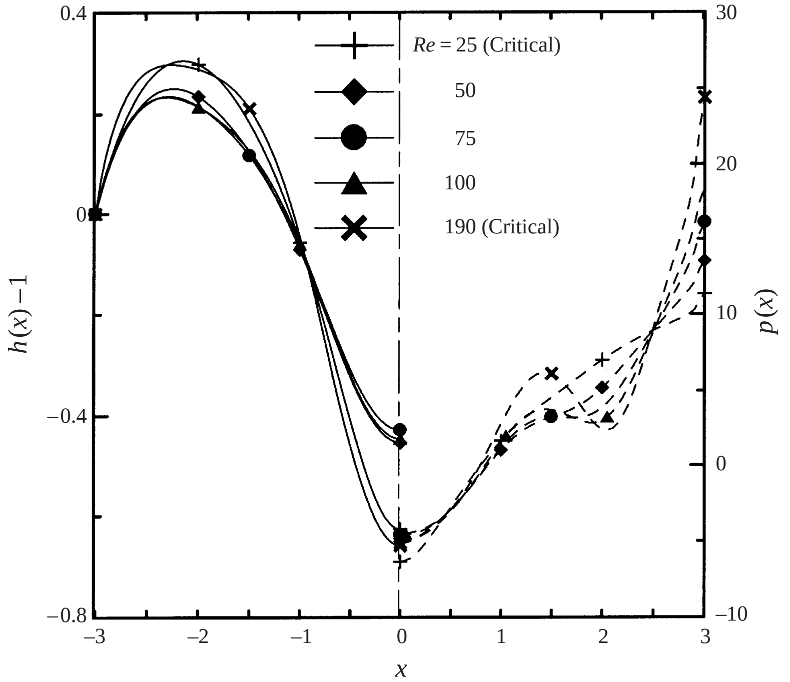

FIGURE 5. The evolution of the interface (left axis) and surface pressure distribution (right axis) as a function of Reynolds number Re for $Ca = 0.1$ and $L = 6$.

is well illustrated in figure 5, which displays the interface shapes for $Ca = 0.1$ and for various values of Re. Variations of the interface shape can be explained by looking at the surface pressure distributions shown in figure 5. The cavity may be subdivided into three types of zones on the basis of the surface pressure distribution. The first type covers a small area in the immediate neighbourhood of the contact point and is characterized by a very large pressure rising rapidly with an increase of Re (which is due to the divergence of pressure at the contact point). The second one covers the area above the vortex centre where a local pressure minimum develops at higher values of Re due to the inviscid character acquired by the vortex core. The third zone covers the middle of the cavity and extends almost over half of its length; the pressure there decreases substantially for lower values of Re but changes insignificantly once the Reynolds number rises above 50. Large pressure in the first zone does not have a major effect on the interface deformation due to the application of the fixed contact point condition. Pressures in the second and the third zones dominate the deformation and their interplay is responsible for the non-monotonic variation of the magnitude of the deformation as Re increases. When Re is small enough (see the curve for $Re = 25$ in figure 5), the pressure is dominated by viscous effects; it has a low minimum at $x = 0$ and rises monotonically with $|x|$. An increase of Re results in the reduction of the pressure force required to overcome viscous friction (see the associated increase of pressure at $x = 0$) and a decrease of pressure above the vortex due to the rise of inertial effects there. The net result is a smaller pressure change along the second and third zones, and thus a smaller interface deformation (see curves for $Re = 50$, 75 and 100 in figure 5). Further increase of Re does not affect the pressure at $x = 0$ but increases the inertial effects leading to the formation of a local pressure maximum

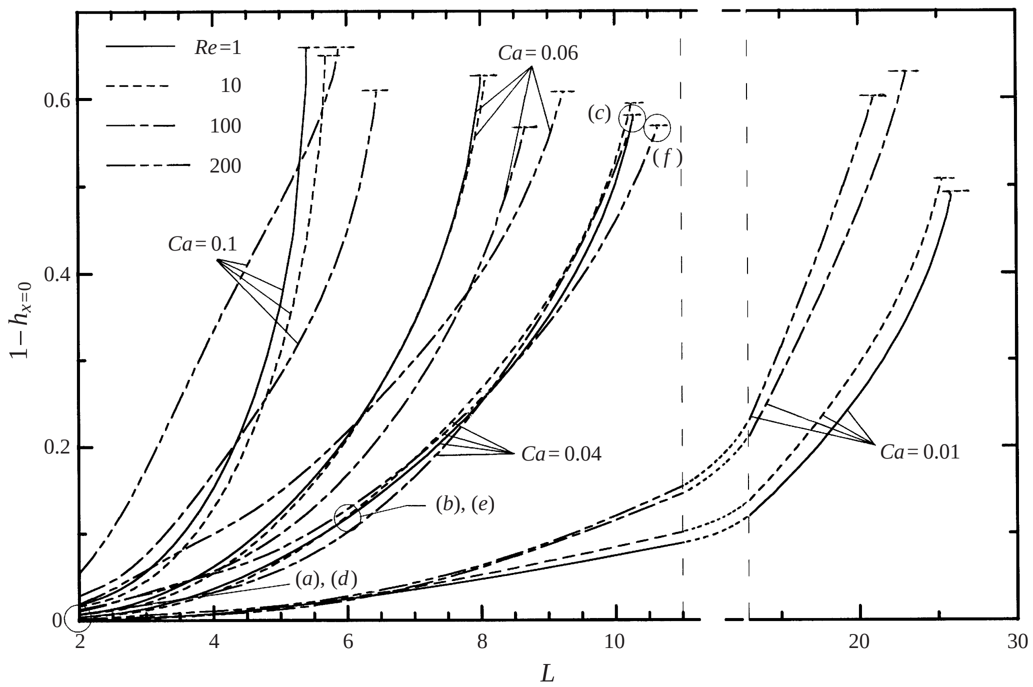

FIGURE 6. Interface deformation at $x = 0$ (maximum deformation) as a function of cavity length L. The flow and deformation patterns corresponding to points (a–f) are shown in figure 7.

on the border between the second and third zones. The resulting increase of the overall pressure change along these zones leads to a higher interface deformation (see the curve for $Re = 190$ in figure 5). This is contrary to the case of the cavity with differentially heated sidewalls (Part 1) where the vortex did not produce a local pressure maximum and thus an increase of Re lead only to a decrease of the interface deformation.

Figure 6 illustrates the effects of the cavity length L (or aspect ratio A) for different values of Re and Ca. It can be seen that as L increases, the deformation increases at a rapidly accelerating rate until no steady solution can be found. We shall demonstrate in the next section that for $L = L_{cr}$ the system reaches a limit point beyond which steady solutions no longer exist. The system will reach the limit point regardless of the value of Ca as long as L is made sufficiently long, which is in agreement with the results of Floryan & Chen (1994). Lower values of Ca result in higher L_{cr}. The dependence of L_{cr} on Re is more complex. For $Ca = 0.01$ an increase of Re results in a decrease of L_{cr}. For $Ca = 0.04$ this relation becomes non-monotonic; an increase of Re from $Re = 1$ to 100 results in a decrease of L_{cr}, while a further increase to $Re = 200$ results in an increase of L_{cr}. At $Ca = 0.06$ this relation is monotonic again, but reversed compared to the situation for $Ca = 0.01$, i.e. an increase of Re corresponds to an increase of L_{cr}. At $Ca = 0.1$ the relation becomes non-monotonic, but this time an increase of Re leads initially to an increase of L_{cr} and then to its eventual decrease when $Re > 100$, which is opposite to what has been observed for $Ca = 0.04$.

Figures 7(a–c) and 7(d–f) illustrate the evolution of the flow and deformation patterns as a function of L for $Ca = 0.04$ and $Re = 1$ and $Re = 200$, respectively. The reader may note that at $Re = 1$ the locations of the vortices are determined

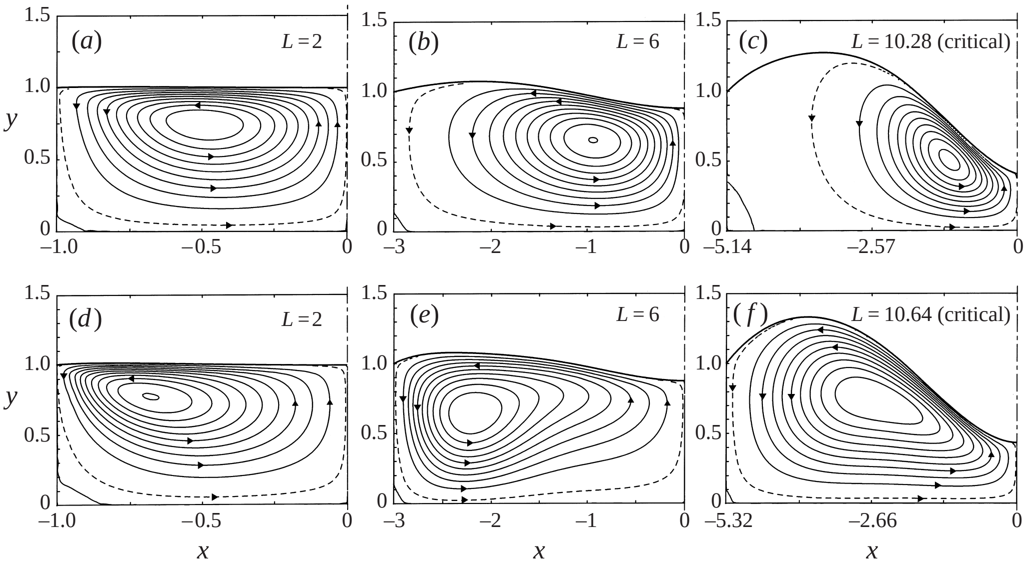

FIGURE 7. The evolution of the flow and deformation patterns as a function of cavity length L for $Ca = 0.04$ and (*a–c*) $Re = 1$, (*d–f*) $Re = 200$. (*a–f*) correspond to points (*a–f*) in figure 6 respectively. Only the left side of the cavity shown due to the symmetry of the flow. Contour lines are shown every 10% of ψ_{max} (solid lines). Dashed lines show 1% of ψ_{max}. In (*a–f*) $|\psi|_{max} = 0.1725$, 1.0222, 0.9402, 0.0955, 0.3947, 0.6944 respectively.

by the location of the point heating, and that the size of the vortex cores (as measured, for example, by the extent of the isoline corresponding to $|\psi/\psi_{max}| = 0.8$) remains approximately constant for $L \geqslant 6$. When $Re = 200$, the vortices appear to be attached to the sidewalls and move apart as the length of the cavity increases, with the size of the vortex cores increasing (and thus becoming more diffused) at the same time. The surface pressure distributions for $Re = 1$ and $Re = 200$ are shown in figure 8. For $Re = 1$ there is a steep negative pressure peak at the point of application of heating. When the length of the cavity increases above $L \geqslant 6$, the pressure approaches a constant value (independent of x) away from the heating area. The pressure distribution is markedly different when $Re = 200$. There are pressure peaks around the contact points and their magnitudes decrease with L. The pressure distribution above the vortex is characterized by the possible appearance of a local pressure minimum when the vortex core acquires inviscid characteristics. Such a local pressure minimum is barely visible for $L = 2$ where it is overshadowed by the large pressure rise at the contact point. This minimum is clearly visible for $L = 6$. For higher cavity lengths, the vortex cores become progressively larger (and more diffused) losing the inviscid characteristics; the associated local pressure drop is still visible for $L = 8$, but hardly recognizable for $L = 10.64$. It is interesting to note that while the character of the surface pressure variations is completely different for $Re = 1$ and $Re = 200$, the final surface deformations and the critical lengths are very similar in both cases. Moreover, the magnitude of the pressure change (along the interface) for both cases is almost the same when $L = L_{cr}$. It appears that when L is sufficiently large, the main factors affecting the magnitude of the deformation are the total pressure change (along the interface) and the length of the cavity. Floryan & Chen (1994) have shown in a much simpler case that even when the pressure change (along the cavity length) remains constant as L increases, the deformation increases proportionally to L^2. Our

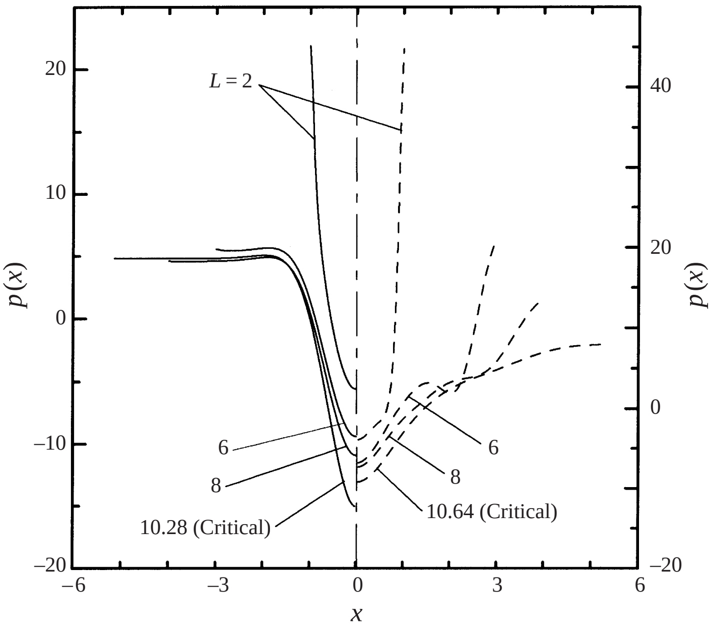

FIGURE 8. The surface pressure distributions as a function of cavity length L for $Ca = 0.04$ and $Re = 1$ (left axis) and $Re = 200$ (right axis).

present results are in qualitative agreement with these conclusions. For $Re = 1$, the pressure change remains essentially constant when the cavity length increases above $L = 6$ (figure 8) and thus the increase of deformation (figure 7*a–c*) is a result of increasing L. For $Re = 200$ the total pressure change decreases as the length increases (figure 8) above $L = 6$. The fact that the corresponding deformation increases shows that the effect of increasing L is much stronger.

It is useful to summarize the above discussion and to point out importance of the cavity length L (or the aspect ratio A) before proceeding to the next subsection. When L is sufficiently small ($L \leqslant 2$ for the range of parameters studied) large interface deformations do not occur due to the strong effect of the fixed contact point conditions. On the other hand, we can reach the limit point even if Ca is fairly small by making the cavity length sufficiently large. Results presented in figure 6 show that for $Ca = 0.01$ the critical length is $L_{cr} \approx 20$–25. Results of other tests show that for $Ca = 0.04$, 0.06, 0.08, 0.1 we have $L_{cr} \approx 10$, 8, 6.5, 5.5, respectively. This clearly shows that one does not require large cavity lengths L before encountering significant interfacial distortions even for fairly small values of Ca. One could conclude that there are two regimes of system response depending on the cavity length. For short cavities, the interface is dominated by the fixed contact points which prevent the appearance of large deformations. For long cavities, the contact points have a minimal effect and the interface is subject to large deformations (including possible rupture). The transition between the 'short cavity' and the 'long cavity' regimes is very rapid and depends on Re and Ca. In the range of parameters studied this transition occurs for $L \in (2, 4)$.

2.2. *Time-dependent response*

We have described in the previous subsection the steady response of the liquid subject to the heating given by (1). We concluded that such a response exists only for a certain

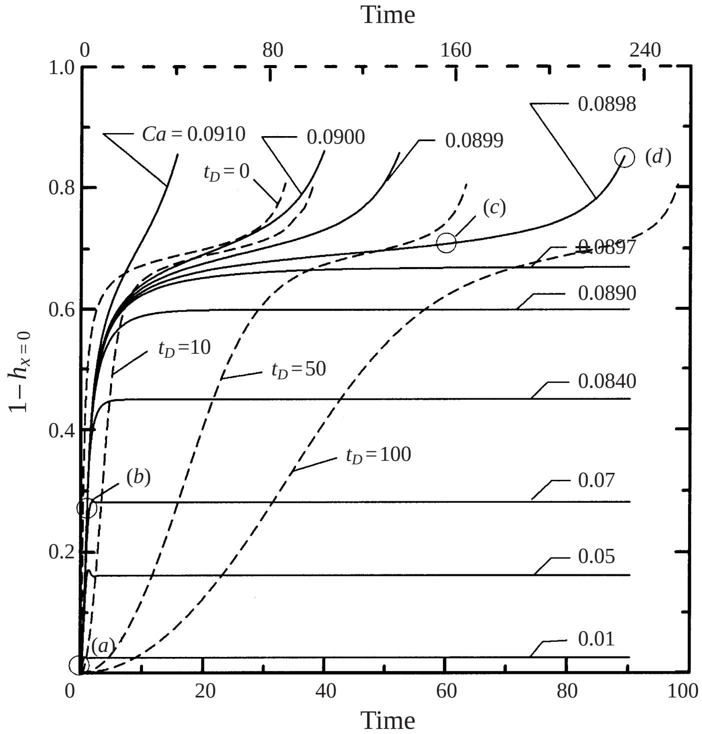

FIGURE 9. Interface deformation at $x = 0$ (maximum deformation) as a function of time for $Re = 1$, $L = 6$, various values of Ca and instantaneous heating (solid lines, lower axis), and for $Re = 1$, $L = 6$, $Ca = 0.0898$ (just above $Ca_{cr} = 0.0879$) and various reductions of the rate of heating (equation 2(*a–c*), dashed lines, upper axis). The flow and deformation patterns corresponding to points (*a–d*) are shown in figure 10.

range of parameter values. In the present subsection we shall describe what happens outside this range. In particular, we shall demonstrate that the critical parameter values determine the limit points of the system. Since the evolution of the system past the limit point could depend on the heating history, we shall consider surface heating in the form

$$T_g(x) = g(x) f_i(t), \quad i = 1, 2, \tag{2a}$$

where $g(x) = 8e^{-x^2}$ and

$$f_1(t) = \mathscr{H}(t), \qquad f_2(t) = 1 - \exp(-t^2/a). \tag{2b,c}$$

Instantaneous heating is described by the Heaviside function $\mathscr{H}(t)$ in (2*b*). A variable rate of heating is described by (2*c*), where the rate of heating is reduced by increasing the value of the constant a. We shall measure the reduction in the rate of heating by introducing the heating delay time t_D defined as the length of time required to reach 90% of the final surface temperature. For example, for $a = 0.4343$, 10.8574, 43.43, 1086, 4343 the heating delay time t_D is equal to 1, 5, 10, 50, 100 time units, respectively.

We shall begin our discussion by considering the effects of the capillary number Ca on the response of the liquid. The reader may recall that we were unable to find any steady solution for $Ca > Ca_{cr}$ (see figure 1). Since the unsteady response is a strong function of Reynolds number Re, we shall carry out the discussion for each of the selected values of Re separately.

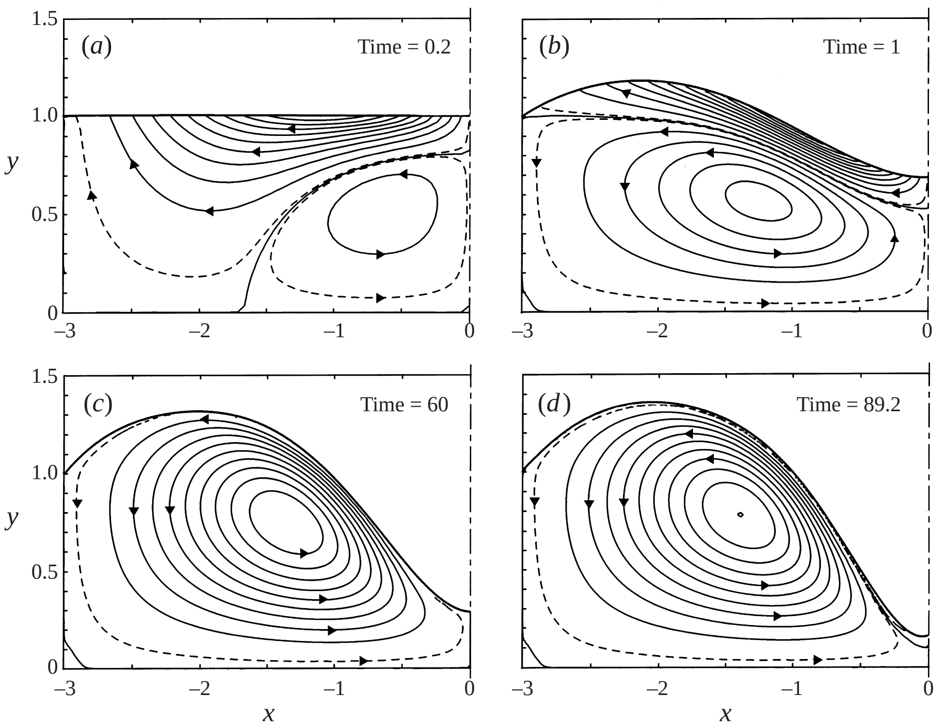

FIGURE 10. The evolution of the flow and deformation patterns as a function of time for $Re = 1$, $L = 6$, $Ca = 0.0898$ (just above $Ca_{cr} = 0.0879$) and instantaneous heating (equations (2*a*, *b*)). (*a*–*d*) correspond to points (*a*–*d*) in figure 9 respectively. Only the left side of the cavity shown due to the symmetry of the flow. Contour lines are shown every 10% of ψ_{max} (solid lines). Dashed lines show 1% of ψ_{max}. In (*a*–*d*) $|\psi|_{max} = 0.07243, 0.15501, 0.19836, 0.20867$ respectively.

Figure 9 displays the time history of the surface deformation at $x = 0$ (maximum deformation) for $Re = 1$, $L = 6$ resulting from instantaneous heating of the liquid (equation (2*a*, *b*)). When $Ca \leqslant Ca_{cr}$ ($Ca_{cr} = 0.0879$), the steady state described in §2.1 is reached for $t > 20$. When $Ca > Ca_{cr}$, a period of rapid initial growth of the deformation (for $t < 5$) is followed by a period of slow growth, after which the growth rapidly re-accelerates. This re-acceleration as well as the absence of any steady state suggest the initiation of a process leading to the rupture of the interface. The length of the slow growth period is a strong function of Ca. For example, for $Ca = 0.0898$ (which is just above Ca_{cr}) this period lasts almost 70 time units, while for $Ca = 0.0910$ it lasts less than 5 units. The evolution of the interface as well as the flow patterns are shown in figure 10 for $Ca = 0.0898$. The reader may note the formation of an internal stagnation point during the initial rapid evolution of the interface immediately after application of the external heating (see, for example, the streamline pattern at $t = 1$ in figure 10). A similar internal stagnation point appears at $t = 89.2$ when the growth of the deformation rapidly accelerates suggesting initiation of the rupture process. The question naturally arises of whether the evolution of the system towards the rupture for $Ca > Ca_{cr}$ is the result of the rapid heating rather than being an intrinsic property of the system. Figure 9 also displays the history of the interface deformation resulting from a reduced rate of heating (equation (2*a*, *c*)) for $Ca = 0.0898$ (just above Ca_{cr}). It can be seen that the qualitative response of the system does not change even for a very slow heating (with the delay time $t_D = 100$). We conclude therefore that Ca_{cr}

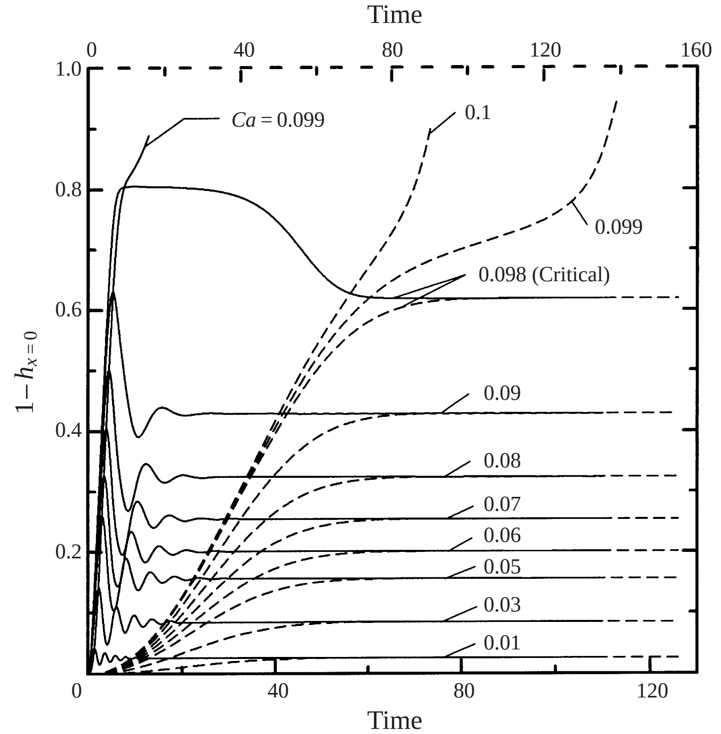

FIGURE 11. Interface deformation at $x = 0$ (maximum deformation) as a function of time for $Re = 20$, $L = 6$ and instantaneous heating (solid lines, lower axis) and a reduced rate of heating with $t_D = 50$ (dashed lines, upper axis).

defines the limit point of the system beyond which no steady states (corresponding to a single continuous interface) exist.

Figure 11 illustrates the response of the liquid in the same cavity ($L = 6$) and subject to an instantaneous heating with the Reynolds number increased to $Re = 20$. When $Ca < Ca_{cr}$ ($Ca_{cr} = 0.098$), the steady state described in § 2.1 is reached for $t > 50$. An initial 'overshoot' of the steady state followed by an oscillatory decaying transient is observed. The magnitude of this 'overshoot' and the amplitude of the oscillatory transient increase while the frequency and the decay rate decrease when Ca increases. A peculiar form of the deformation is observed for $Ca \approx Ca_{cr}$ where the deformation initially rapidly increases to a level much higher than the one corresponding to the steady state, then it remains almost stationary for about 20 time units, and afterwards it slowly decreases to the steady-state level. When $Ca > Ca_{cr}$, the deformation keeps rapidly increasing without any of the slowing down observed for $Re = 1$. This rapid growth as well as the absence of any steady state suggest that we observe the initiation of a process leading to the rupture of the interface. Figure 11 illustrates the fact that we can eliminate the initial 'overshoot' and the oscillatory transient, as well the peculiar 'hump' in the evolution of the deformation for $Ca \approx Ca_{cr}$, by slowing down the heating. One can also see that no steady state can be reached for $Ca > Ca_{cr}$, even with very slow heating.

Figure 12 illustrates the response of the liquid in the same cavity ($L = 6$) subject to the same heating with the Reynolds number increased to $Re = 100$. Comparison of figures 11 and 12 shows that such an increase of the Reynolds number results

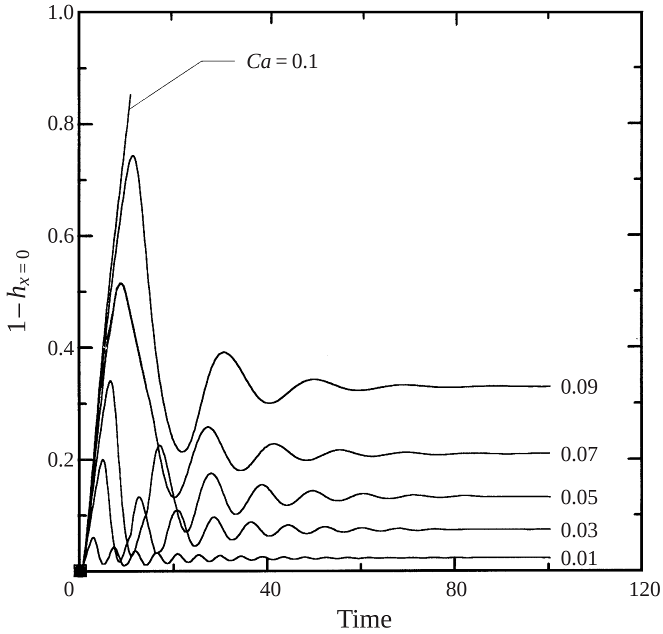

FIGURE 12. Interface deformation at $x = 0$ (maximum deformation) as a function of time for $Re = 100$, $L = 6$ and instantaneous heating (equations (2a, b)).

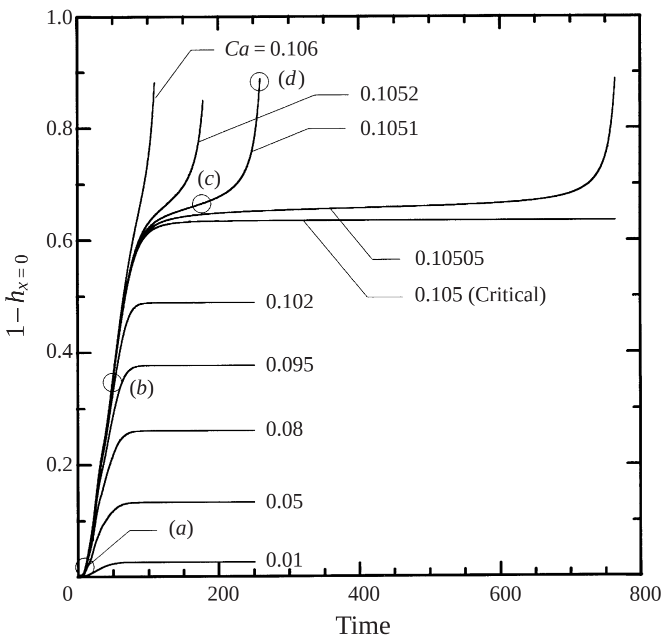

FIGURE 13. Interface deformation at $x = 0$ (maximum deformation) as a function of time for $Re = 100$, $L = 6$ and a reduced heating rate with $t_D = 50$. The flow and deformation patterns corresponding to points (a–d) are shown in figure 14.

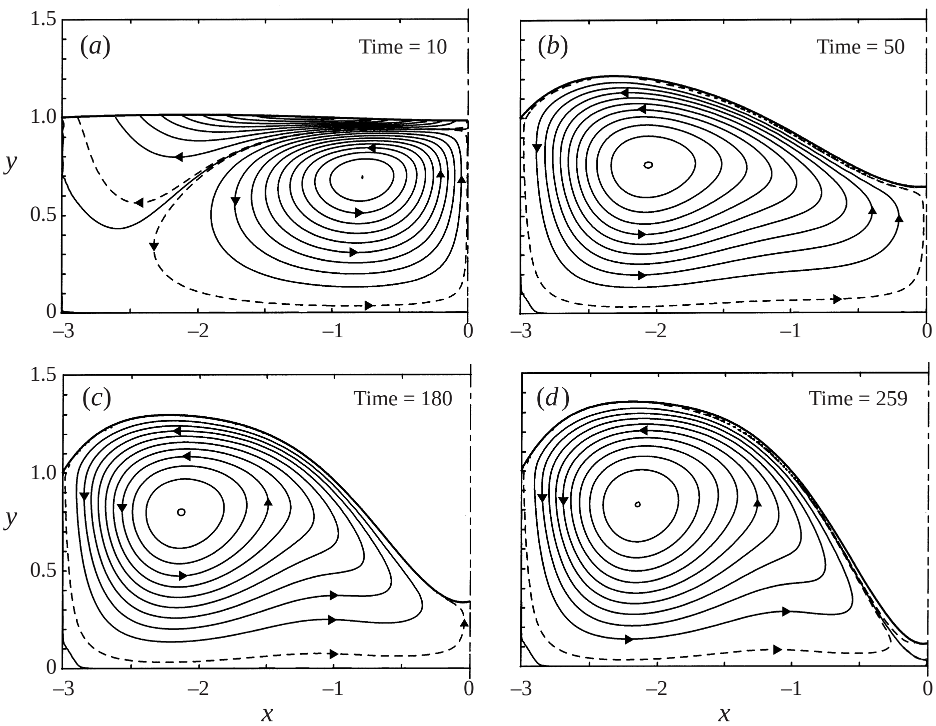

FIGURE 14. The evolution of the flow and deformation patterns as a function of time for $Re = 100$, $L = 6$, $Ca = 0.1051$ (just above $Ca_{cr} = 0.105$) and a reduced heating rate with $t_D = 50$. (*a–d*) correspond to points (*a–d*) in figure 13 respectively. Only the left side of the cavity shown due to the symmetry of the flow. Contour lines are shown every 10% of ψ_{max} (solid lines). Dashed lines show 1% of ψ_{max}. In (*a–d*) $|\psi|_{max} = 0.54311 \times 10^{-2}$, 0.11529, 0.14499, 0.15074 respectively.

in a large increase of the initial overshoot of the steady state and a much stronger and longer lasting oscillatory transient. The frequency of the oscillations increases while their amplitudes decrease with a reduction of *Ca*. All transients decay in less than 80 time units. We were unable to reach the steady-state solution described in § 2.1 for $Ca = 0.1 < Ca_{cr}$ ($Ca_{cr} = 0.105$). The available results suggest that the large initial overshoot of the interface deformation associated with such a rapid heating triggers an early (i.e. before the critical conditions determined on the basis of analysis of steady solutions are reached) interface rupture process. Figure 13 illustrates the fact that the reduction of the rate of heating eliminates the oscillatory transients and, indeed, we can reach steady state even for $Ca = Ca_{cr}$. The reduction in the heating rate has to be, however, more pronounced than the one required for $Re = 20$. If $Ca > Ca_{cr}$, no steady state can be reached and the system evolves towards the rupture regardless of the significant reduction of heating rate. Figure 14 illustrates the evolution of the interface and the flow patterns for $Ca = 0.1051$ (just above Ca_{cr}) obtained with the same heating rate as in figure 13. One can observe the appearance of the internal stagnation point in the centre of the cavity at $t = 259$ which characterizes the initiation of the rupture process. On the basis of these and other tests we conclude that Ca_{cr} defines a limit point.

To conclude the discussion of the effect of *Re*, we would like to draw the reader's attention to the curve corresponding to $Ca = 0.1$ in figure 3(*b*). This curve suggests that the range of *Re* for which steady solutions exist is limited from above as well

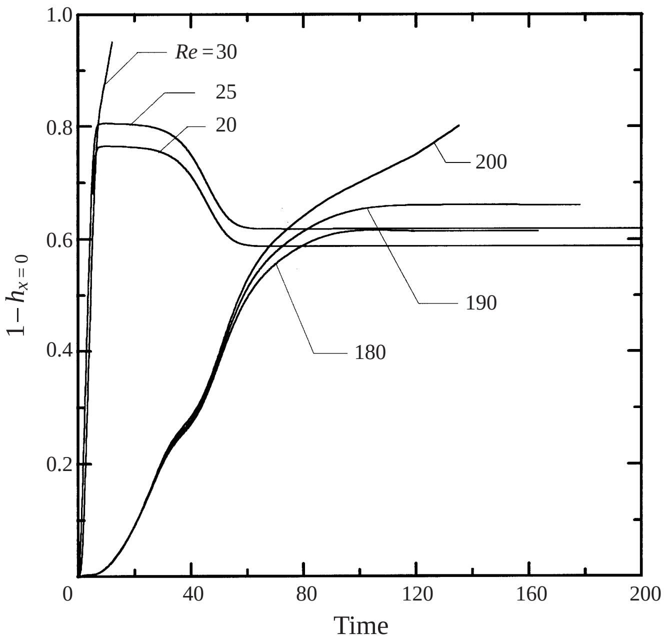

FIGURE 15. Interface deformation at $x = 0$ (maximum deformation) as a function of time for $Ca = 0.1$, $L = 6$, instantaneous heating for $Re = 20$, 25, 30, and a reduced heating rate with $t_D = 50$ for $Re = 180$, 190, 200.

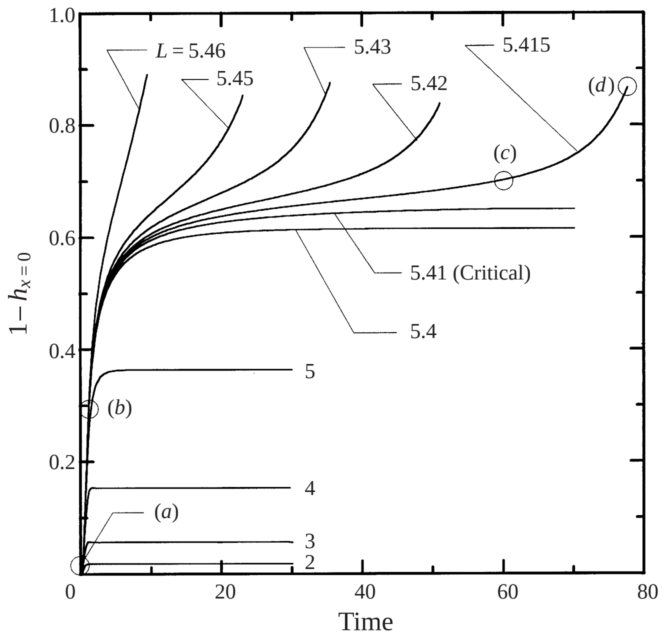

FIGURE 16. Interface deformation at $x = 0$ (maximum deformation) as a function of time for $Re = 1$, $Ca = 0.1$ and instantaneous heating (equation (2a, b)). The flow and deformation patterns corresponding to points (a–d) are shown in figure 17.

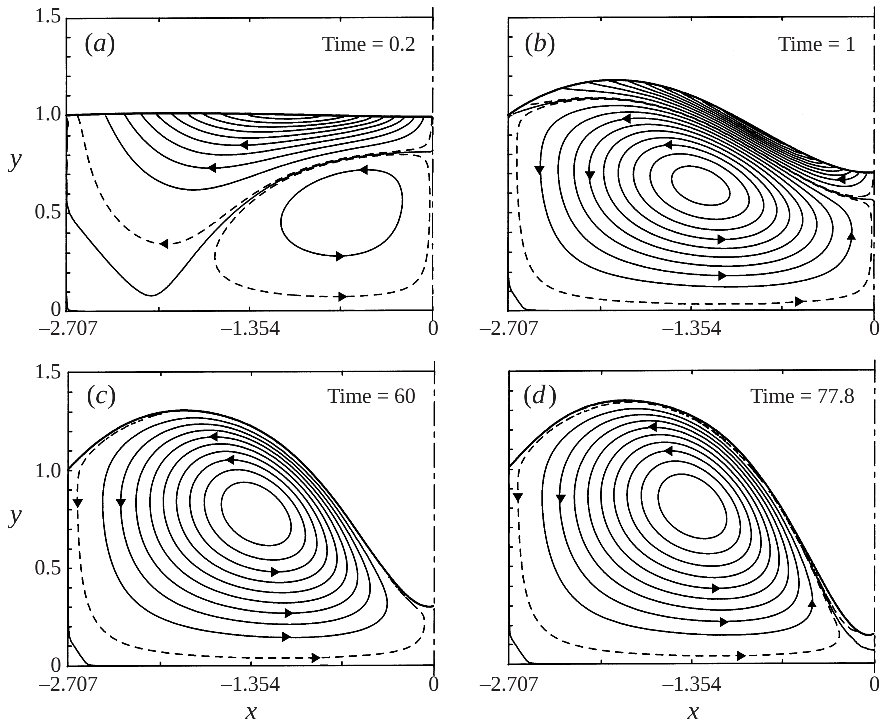

FIGURE 17. The evolution of the flow and deformation patterns as a function of time for $Re = 1$, $Ca = 0.1$, $L = 5.415$ (just above $L_{cr} = 5.41$) and instantaneous heating. (*a–d*) correspond to points (*a–d*) in figure 16 respectively. Only the left side of the cavity shown due to the symmetry of the flow. Contour lines are shown every 10% of ψ_{max} (solid lines). Dashed lines show 1% of ψ_{max}. In (*a–d*) $|\psi|_{max} = 0.06888, 0.12164, 0.23321, 0.24974$ respectively.

as from below. Results shown in figure 15 demonstrate that indeed the system has limit points at $Re_{cr,b} \approx 25$ and $Re_{cr,a} \approx 190$. The calculations for $Re = 180, 190, 200$ had to be carried out with the reduced heating rate ($t_D = 50$) for the same reason as explained in the previous paragraph.

The last issue that we wish to discuss is the question of the effects of the cavity length L. We were unable to find steady solutions for $L > L_{cr}$ (see figure 6). Figure 16 displays the time history of the surface deformation at $x = 0$ for $Re = 1$, $Ca = 0.1$ resulting from instantaneous heating (equation (2*a*, *b*)). When $L < L_{cr}$ ($L_{cr} = 5.41$), the steady state described in § 2.1 is reached for $t > 20$. When $L > L_{cr}$, a period of rapid initial growth of the deformation (for $t < 5$) is followed by a period of slow growth, after which the growth rapidly re-accelerates. The form of the growth as well as the absence of any steady state suggest the initiation of a process leading to the rupture of the interface. The length of the period of slow growth preceding rapid re-acceleration is a strong function of L. For example, for $L = 5.415$ (which is just above L_{cr}) this period lasts 60 time units, while for $L = 5.46$ it lasts less than 7 units. The evolution of the interface as well as the flow patterns are shown in figure 17 for $L = 5.415$ (just above L_{cr}). The reader again may note the formation of very similar internal stagnation points during the initial period of rapid growth (at $t = 1$) and during the rapid growth associated with the rupture (at $t = 77.8$). Similar results can be obtained for higher values of Re. On the basis of these and other tests we conclude that L_{cr} defines a limit point of the system beyond which no steady states (corresponding to a single continuous interface) exist.

3. Conclusions

We have investigated Marangoni convection in a cavity subject to (concentrated) point heating, including the complete interface deformation effects. Detailed results were presented for the case of the Marangoni number $Ma = 0$ (dominant conductive heat transport; Prandtl number $Pr = 0$) and the Biot number $Bi = \infty$ (very high heat transfer coefficient at the interface).

The results show that steady convection exists for a limited range of the Reynolds numbers Re bounded from below and from above, and for capillary numbers Ca and cavity lengths L smaller than certain critical values. The critical values Re_{cr}, Ca_{cr} and L_{cr} are mutually dependent. When any of Re, Ca, or L approaches its respective critical value, the magnitude of the interface deformation increases rapidly, with the interface approaching (as a function of this particular parameter) the bottom of the cavity. Such interface evolution implies initiation of a process leading to the rupture of the interface (and formation of a dryout at the bottom of the cavity) when any of the Re, Ca, or L traverses its critical value. The physical character of the process that limits the existence of steady convection is different from the case of the cavity with differentially heated sidewalls, where the limiting factor involves the interface becoming tangential to the hot wall. It is worth noting that in the present case the increased viscous friction is responsible for the increased deformation when Re decreases, while rearrangement of the pressure field associated with the vortex dynamics is responsible for the increase of the deformation when Re increases. Vortex dynamics in the case of heated sidewalls rearranges the pressure field differently, always leading to reduction of the deformation when Re increases.

The convection pattern is symmetric with respect to the middle of the cavity and consists of two dominant vortices, each being the mirror image of the other. When Re increases, the centres of the vortices move apart and towards the sidewalls, with their cores attaining inviscid characteristics for sufficiently large values of Re. The inviscid character of the vortex core manifests itself through the creation of a local pressure minimum at the interface above the core and a local flattening (or depression) of the interface. When cavity length increases, the location of the vortex centres is determined by the location of the point heating if Re is very small. For high values of Re the centres of the vortices remain attached to their respective walls and move away from the centre of the cavity when the cavity length increases. At the same time, the size of the vortex core increases (thus becoming more diffused). If this core has had an inviscid character in a short cavity, it loses this character when the cavity length becomes large enough.

Unsteady analysis shows that the response of the liquid depends on the rate of heating. For Re, Ca, and L outside the ranges limited by the critical values Re_{cr}, Ca_{cr} and L_{cr}, the deformation increases continuously in time from the moment of application of the heating until the interface approaches the bottom of the cavity so closely that the calculations cannot be continued. For Re, Ca, and L very close to their respective critical values, the time history of the deformation consists of a rapid initial growth (just after the application of the heating) followed by a characteristic slow down. The existence of this slow down suggests that the specified conditions are very close to those under which a steady solution exists. The end of the growth process consists of a rapid re-acceleration of the growth suggesting initiation of the rupture process. The form of the interface growth process shows that Re_{cr}, Ca_{cr} and L_{cr} define the limit points for the system. The location of the limit points in the parameter space is sensitive to the rate of heating for a certain range of parameters. The presence of potentially very strong transient effects is responsible for this sensitivity. These transients can be effectively controlled by reducing the rate of heating.

This work was supported by the NSERC of Canada.

REFERENCES

Batchelor, G. K. 1956 *J. Fluid Mech.* **1**, 177–190.
Burelbach, J. P., Bankoff, S. G. & Davis, S. H. 1990 *Phys. Fluids* A **2**, 322–333.
Floryan, J. M. & Chen, C. 1994 *J. Fluid Mech.* **277**, 303–329.
Hamed, M. & Floryan, J. M. 2000 *J. Fluid Mech.* **405**, 79–110.
Rivas, D. 1991 *Phys. Fluids* A **3**, 280–291.
Tan, M. J., Bankoff, S. G. & Davis, S. H. 1990 *Phys. Fluids* A **2**, 313–321.